Non-visual light modulates behavioral memory and gene expression in *C. elegans*

Zhijian Ji[1, §], Bingying Wang[1, §], Rashmi Chandra[1, §], Junqiang Liu[1, §], Supeng Yang[1, 2], Yong Long[3], Michael Egan[1, 2], Noelle L'Etoile[4], Dengke K. Ma[1, 5, 6, *]

[1]Cardiovascular Research Institute, University of California San Francisco, San Francisco, CA 94158, USA.

[2]Department of Molecular Cell Biology, University of California, Berkeley, Berkeley, CA 94720, USA.

[3]Key Laboratory of Breeding Biotechnology and Sustainable Aquaculture, Institute of Hydrobiology, Chinese Academy of Sciences, Wuhan 430072, China.

[4]Department of Cell and Tissue Biology, University of California San Francisco, San Francisco, CA 94158, USA.

[5]Department of Physiology, University of California San Francisco, San Francisco, CA 94158, USA.

[6]Innovative Genomics Institute, University of California, Berkeley, Berkeley, CA 94720, USA.

[§] Equal contribution

*Correspondence: Dengke.Ma@ucsf.edu

Abstract

Visible light influences a range of physiological processes, yet how animals respond to it independently of the visual system remains largely unknown. Here, we uncover a previously undescribed light-induced transcriptional pathway that modulates behavioral plasticity in *C. elegans*, a roundworm without eyes. We demonstrate that ambient visible light or controlled-intensity visible-spectrum LED activates an effector gene *cyp-14A5* in non-neuronal tissues through the bZIP transcription factors ZIP-2 and CEBP-2. Light induction of *cyp-14A5* is more prominent at shorter wavelengths but is independent of the known blue light receptors LITE-1 and GUR-3 in *C. elegans*. This bZIP-dependent genetic pathway in non-neuronal tissues enhances behavioral adaptability and olfactory memory, suggesting a body-brain communication axis. Furthermore, we use the light-responsive *cyp-14A5* promoter to drive ectopic gene expression, causing synthetic light-induced sleep and rapid aging phenotypes in *C. elegans*. These findings advance our understanding of light-responsive mechanisms outside the visual system and offer a new genetic tool for visible light-inducible gene expression in non-neuronal tissues.

Introduction

Visible light is crucial for image formation and regulating various physiological processes through the visual system, yet how animals respond to ambient light independently of sight remains poorly understood. Recent studies have uncovered diverse non-visual photoreception mechanisms that modulate a range of biological processes, from circadian rhythms to stress responses and metabolic homeostasis(Andrabi et al., 2023; Cronin and Johnsen, 2016; Do and Yau, 2010; Van Gelder, 2008). These mechanisms often involve specialized light-sensitive proteins, such as opsins and cryptochromes, widely expressed in body locations, including the skin, brain, and peripheral organs. For example, mammalian melanopsin-expressing retinal ganglion cells play critical roles in systemic light responses largely independent of image formation(Berson et al., 2002; Hattar et al., 2003; Lucas et al., 2003; Shi et al., 2024). In the nematode roundworm *C. elegans*, blue light photoreception requires the light-activated ion channels LITE-1 and GUR-3 in specific neurons, influencing aversive behaviors and cellular physiology(Bhatla and Horvitz, 2015a, 2015b; Edwards et al., 2008; Gong et al., 2016; Hanson et al., 2023). Visible light irradiation can also generate photo-oxidative reactive oxygen species in animals(De Magalhaes Filho et al., 2018; Liebel et al., 2012; Mahmoud et al., 2010). Despite these advances, the molecular pathways and physiological outcomes of non-visual light sensing and responses remain understudied, raising intriguing questions about the mechanistic basis and functional implications of light as an environmental cue beyond vision.

We previously studied how genes encoding cytochrome P450 (CYP) proteins respond to and mediate effects of exposure to environmental stresses in *C. elegans*(Keller et al.,

61 2014; Ma et al., 2013). Among various transcriptional reporters we generated for CYP-
62 encoding genes to monitor environmental regulation, we serendipitously discovered that
63 the *cyp-14A5* promoter-driven GFP expression is particularly sensitive to ambient visible
64 light exposure. Building upon this initial finding, we conduct transcriptome profiling to
65 identify light-inducible genes in addition to *cyp-14A5*, determine key transcriptional
66 regulators of *cyp-14A5*, and show that the light-inducible CYP-14A5 promotes
67 behavioral plasticity and olfactory memory in *C. elegans*. The findings also provide a
68 genetic tool to use light-inducible *cyp-14A5* promoter to flexibly and ectopically drive
69 gene expression.

70

71 **Results**

72 **Light activates expression of *cyp-14A5* and other genes in *C. elegans***

73 Cytochrome P450 proteins comprise a highly conserved superfamily of heme-containing
74 monooxygenases critical for metabolizing endogenous and xenobiotic
75 compounds(Denisov et al., 2005). We constructed transcriptional reporters for genes
76 encoding CYPs in *C. elegans* and found that *cyp-14A5p::GFP* was drastically up-
77 regulated by bright-field transmission light from a microscope inadvertently left on
78 overnight. Using controlled light versus dark conditions, we confirmed the finding from
79 an integrated *cyp-14A5p::GFP* reporter and observed its robust widespread GFP
80 expression in many tissues induced by moderate-intensity (500-3000 Lux, 16-48 hr
81 duration) LED light exposure (**Fig. 1A**). The level of GFP expression increased
82 proportionally with both light intensity and duration (**Fig. 1B**), the condition of which

83 does not impact ambient temperature (**Fig. S1A-S1D**). Other common stresses,
84 including transient 32 ^{o}C heat shock, constant 24-hr hypoxia or starvation did not
85 apparently induce *cyp-14A5p::GFP* (**Fig. S1E-S1H**). Together, these data suggest that
86 *cyp-14A5p::GFP* induction is finely tuned to ambient light conditions.

87 To determine CYP-14A5 protein expression pattern, we constructed a translational GFP
88 reporter (*cyp-14A5p::cyp-14A5::GFP*) and observed robust light-induced expression of
89 CYP-14A5::GFP in many of the non-neuronal tissues, including the pharynx, hypoderm
90 and intestine (**Fig. 1C**). The transcriptional reporter exhibited similar patterns of non-
91 neuronal GFP induction by light (**Fig. 1A**). The translational reporter reveals the CYP-
92 14A5::GFP pattern indicative of the endoplasmic reticulum structure (**Fig. 1C**),
93 consistent with the known subcellular localization of most CYPs to ER
94 membranes(Neve and Ingelman-Sundberg, 2010).

95 To explore how eyeless *C. elegans* responds to ambient visible light independently of a
96 visual system, we conducted transcriptomic profiling by RNA-seq in *C. elegans* exposed
97 to controlled light or dark conditions. We found that defined visible light exposure (1500
98 Lux, 24 hr duration) to a synchronized population of young adults (24 hrs post L4)
99 triggered a robust genome-wide transcriptional response, including 7902 genes
100 differentially regulated (adjusted P value < 0.05, **Fig. 1D** and **Table S1**). Among these,
101 *cyp-14A5* was one of the most strongly upregulated genes (**Fig. 1E**). Gene ontology
102 (GO) analysis of the light-induced transcriptome reveals their significant enrichment in
103 several pathways, including transmembrane signaling, pathogen and stress responses,
104 protein phosphorylation, cellular homeostasis and metabolisms (**Fig. S2**).

105 **ZIP-2 and CEBP-2 are essential for light-induced transcriptional responses**

106 We next investigated the molecular regulators driving *cyp-14A5* activation in response
107 to light. To test if it requires previously identified blue-light receptors LITE-1 or GUR-3,
108 we crossed the *cyp-14A5p::GFP* reporter with *lite-1* and *gur-3* double loss-of-function
109 mutants. Surprisingly, light-induced GFP expression was preserved in *lite-1gur-3* double
110 mutants, indicating that *cyp-14A5* activation operates through an alternative, non-visual
111 light-sensing mechanism (**Fig. 2A**). Prolonged photonic light exposure may also cause
112 photo-oxidation of DNA and genotoxicity, leading to DNA damage and ATM protein-
113 dependent check points and transcriptional responses(Ciccia and Elledge, 2010; De
114 Magalhaes Filho et al., 2018; Schuch et al., 2017). However, loss of the DNA damage
115 sensor ATM-1 did not apparently affect light-induced *cyp-14A5p::GFP* (**Fig. 2A**). These
116 findings underscore the existence of a novel light-responsive pathway in *C. elegans*,
117 distinct from previously characterized photoreceptive systems.

118 To identify transcriptional regulators driving *cyp-14A5* activation in response to light, we
119 adopted an RNAi-based screening strategy, focusing initially on approximately 400
120 genes encoding transcription factors, including those responding to various types of
121 stresses. Knockdown of the expression of genes encoding TF from a previously
122 assembled RNAi library or selected for mediating various common stress responses
123 (hypoxia, oxidative stress, heat shock etc.) did not appear to affect *cyp-14A5* activation
124 in response to light (**Fig. 2B**). Interestingly, we identified from such screen two bZIP-
125 type transcription factors, ZIP-2 and CEBP-2, as critical mediators of light-induced *cyp-*
126 *14A5* transcription (**Fig. 2B**). Knockdown or genetic ablation of either *zip-2* or *cebp-2*

127 abolished light-induced *cyp-14A5p::GFP* expression (**Fig. 2B, 2C**). ZIP-2 and CEBP-2
128 have been previously identified(Dunbar et al., 2012; Estes et al., 2010; Kniazeva and
129 Ruvkun, 2025; Reddy et al., 2016) to cooperate in a regulatory complex and mediate
130 transcriptional responses to translational inhibition caused by the bacterial pathogen
131 *Pseudomonas aeruginosa* PA14. In these studies, the *irg-1*p::GFP transcriptional
132 reporter was robustly activated by PA14 as a well-established target for ZIP-2 and
133 CEBP-2. Interestingly, we found *irg-1*p::GFP was not activated by the same light
134 condition (1500 Lux, 24 hrs) that reliably induced *cyp-14A5*p::GFP (**Fig. 2D**). Although
135 ZIP-2 can be activated by pathogen stresses through ribosomal inhibition and
136 subsequent selective ZIP-2 translation(Dunbar et al., 2012; Estes et al., 2010; Kniazeva
137 and Ruvkun, 2025; Reddy et al., 2016), our results suggest the specific roles of ZIP-2 in
138 mediating light-induced *cyp-14A5* but not *irg-1* reporter expression, suggesting the
139 involvement of additional stress context-specific factors in these processes.

140 We further explored conditions and mechanisms leading to light-induced *cyp-*
141 *14A5p::GFP*. To test potential effects of ultraviolet (UV) irradiation from our visible light
142 LED, we used a UV-masking shield to block UV irradiation. However, this did not affect
143 visible LED light-induced *cyp-14A5p::GFP* expression (**Fig. 2E**). In addition, we found
144 that the LED light exposure of equal intensities (1500 Lux, 24 hrs) but at different
145 wavelengths (red, green, blue) led to differential *cyp-14A5p::GFP* expression (**Fig. 2F,**
146 **2G**), showing stronger effects of shorter wavelengths in the visible-light spectrum. A
147 pseudo-open reading frame (uORF) in the 5' untranslated region (UTR) of *zip-2* mRNA
148 inhibits the ribosomal translation of the ZIP-2 main open reading frame (mORF) in the
149 context of PA14 pathogen exposure(Dunbar et al., 2012). However, constitutive

150 expression of *zip-2* uORF by the *rpl-28* promoter did not affect light-induced *cyp-*
151 *14A5p::GFP* (**Fig. 2H**). Furthermore, a CRISPR phospho-site knock-in mutation of *eif-*
152 *2alpha(S49A)* did not affect global translation(Ma et al., 2023), yet abolished light-
153 induced *cyp-14A5p::GFP* (**Fig. 2I**). As the eukaryotic eIF2alpha complex facilitates
154 translational switch from uORF to mORF upon stress-induced ribosomal stall at
155 uORF(Brito Querido et al., 2024; Costa-Mattioli and Walter, 2020; Mir et al., 2024),
156 these results suggest that it is the *zip-2* uORF translational inhibition, not the uORF
157 protein product function, that mediates visible light-increased ZIP-2 translation and *cyp-*
158 *14A5p::GFP* expression (**Fig. 2J**).

159 **Light-induced CYP-14A5 enhances behavioral memory**

160 Although EIF-2alpha and ZIP-2/CEBP-2 functions appear essential for light-induced up-
161 regulation of *cyp-14A5*, the *zip-2* or *cyp-14A5* loss-of-function null mutants show no
162 apparent body-size, morphological, feeding, defecation or developmental defects under
163 dark or LED light treatment (1500 Lux for 16 or 24 hrs) conditions (**Fig. S3**). These data
164 suggest that transient visible light exposure or light-induced *cyp-14A5* activation by ZIP-
165 2 does not broadly impact development, aging or physiology, unlike long-term visible
166 light exposure, which has been shown to robustly shorten lifespans in *C. elegans*(De
167 Magalhaes Filho et al., 2018).

168 The lack of obvious morphological and basal behavioral defects led us to explore
169 whether light exposure influences other aspects of *C. elegans* biology, particularly
170 behavioral plasticity and associative memory formation that might require integration of
171 body physiology. Specifically, we chose a learning paradigm in which animals learn to

172 avoid an innately attractive odor butanone after it is paired with aversive
173 stimuli(Chandra et al., 2023; Kauffman et al., 2010). *C. elegans* can consolidate this
174 learning into a long-lasting memory for up to 16 hours once the repetitive training is
175 followed by sleep and recovery post learning(Chandra et al., 2023). Using this
176 conditioning protocol (**Fig. 3A**), we observed that animals exposed to ambient light
177 (approximately 500–1000 Lux) during olfactory associative learning and recovery
178 exhibited significantly enhanced memory retention compared to those maintained in
179 darkness (**Fig. 3B**). To pinpoint the critical period for light exposure, we deprived
180 animals of light in two-hour intervals immediately post learning. Interestingly, light
181 deprivation during the first 2–4 hours post learning resulted in markedly impaired
182 memory retention (**Fig. 3C**). These results suggest that environmental light exposure
183 enhances aversive cue association post learning and is not required for learning itself
184 but is required post learning concurrent with sleep for consolidation of memory(Chandra
185 et al., 2023).

186 Does the light-modulated behavioral memory consolidation require light activation of the
187 ZIP-2 pathway? To address this question, we examined the behavioral memory of two
188 independent *zip-2* deletion mutants as compared to wild type (*cebp-2* mutants are
189 pleiotropically sick and thus not included). We found that both the *ok3730* and *tm4246*
190 deletion mutations of *zip-2* caused significantly impaired memory consolidation but not
191 learning (**Fig. 3D**). Strikingly, the loss-of-function mutation of *cyp-14A5*, but not *F43C1.7*
192 (another ZIP-2 target gene induced by visible light), also impaired memory retention as
193 *zip-2* (**Fig. 3E**), indicating a crucial role of the ZIP-2/CYP-14A5 regulatory axis in
194 mediating light-modulated memory consolidation. To further delineate the role of CYP-

195 14A5, we performed tissue-specific rescue experiments in the behavioral memory
196 assay. We found that hypoderm-specific expression of *cyp-14A5* restored the
197 behavioral memory in the *cyp-14A5* mutant (**Fig. 3F**). We observed similar degrees of
198 rescue by two independently derived lines expressing hypoderm-specific *dpy-7p::cyp-*
199 *14A5* transgenes. These findings strongly suggest that hypodermal induction of CYP-
200 14A5 by ZIP-2 plays a central role in mediating light-modulated behavioral memory.

201 **The *cyp-14A5* promoter as a versatile tool for light-inducible gene expression**

202 The light-responsive nature of the *cyp-14A5* promoter prompted us to explore its
203 potential as a tool for controlling gene expression. We generated synthetic constructs
204 driving the expression of diverse effectors under the *cyp-14A5* promoter to confer
205 striking organismal phenotypes. We previously found that *zip-10* expression promotes
206 organismal phenoptosis(Pandey and Ma, 2022; Wang et al., 2023). Driven by the *cyp-*
207 *14A5* promoter, light-induced *zip-10* expression indeed caused a robust light-dependent
208 rapid aging or phenoptosis-like phenotype with markedly shortened median and
209 maximal lifespans (**Fig. 4A-4D**). We confirmed that LED light exposure markedly
210 induced *zip-10* expression, as evidenced by robust ZIP-10-tagging mCherry
211 fluorescence in major non-neuronal tissues of transgenic animals, only after light (1500
212 Lux, 24 or 48 hrs) exposure (**Fig. 4C**).

213 To test organismal behavioral outcomes, we expressed *nlp-22* under the *cyp-14A5*
214 promoter. *nlp-22* was previously identified as a sleep-promoting
215 neuropeptide(Bringmann, 2018; Nelson et al., 2013; Van der Auwera et al., 2020),
216 overexpression of which can cause drastic reduction of pumping and locomotion speed,

217 characteristic of sleep behaviors in *C. elegans*. We found that *cyp-14A5p::nlp-22* can
218 indeed trigger striking behavioral quiescence upon light exposure (1500 Lux, 24 or 48
219 hrs), as quantified by pumping rates, bending frequencies and locomotion speed (**Fig.**
220 **4E-4G)**. Quantitative analysis by WormLab reveals that the behavioral quiescence
221 induced by *nlp-22* corresponded to characteristic bouts of sleep **(Fig. S4**). These proof-
222 of-concept studies demonstrate that the *cyp-14A5* promoter enables light-dependent
223 ectopic induction of gene expression, offering a flexible tool for probing gene function,
224 studies of organismal biology, behaviors and synthetic physiology applications.

225

226 **Discussion**

227 Our findings uncover a previously unknown light-induced transcriptional pathway in *C.*
228 *elegans* that operates independently of known visual light receptors. Our study also
229 establishes a functional link between ambient light and behavioral plasticity through a
230 ZIP-2/CYP regulatory axis. The discovery of this pathway and its organismal functions
231 opens exciting avenues for understanding body-brain communication and how
232 environmental cues such as light can shape physiological and behavioral processes.

233 The specificity of this pathway is particularly intriguing, as *cyp-14A5* is robustly induced
234 by light at wavelength and intensity that do not apparently alter ambient temperature
235 (**Fig. S1**). Previous studies identified *cyp-14A5* as one of many genes moderately
236 regulated by bacterial pathogens(Sinha et al., 2012; Troemel et al., 2006; Wong et al.,
237 2007), yet the classic pathogen-inducible gene reporter *irg-1p::GFP* was not apparently
238 activated by light conditions that induced *cyp-14A5*p::GFP. This specificity raises

important questions about how ZIP-2 and *cyp-14A5* are selectively activated by light, or to different degrees. Given the crucial roles of ZIP-2 and eIF2alpha we discovered for light-induced expression of *cyp-14A5* and the established role of the uORF at the 5' untranslated region of *zip-2* RNA in ZIP-2 regulation(Dunbar et al., 2012), it is plausible that light may regulate ZIP-2 translation by *zip-2* RNA photo-oxidation at specific sites, eIF2alpha phosphorylation and specialized ribosomal signaling(D'Orazio and Green, 2021; Genuth and Barna, 2018; Sinha et al., 2024). Further investigation into the upstream signaling events and the molecular sensors linking light exposure to ZIP-2/CEBP-2 activation is warranted.

Our behavioral assays demonstrate that light exposure enhances olfactory associative memory, providing direct evidence for the functional relevance of light-induced *cyp-14A5* expression. Interestingly, light exposure appears to exert its effects during a specific temporal window hours following learning, suggesting that light-induced transcriptional changes post learning play a key role in memory consolidation. The discovery of *cyp-14A5* as a key effector in this pathway also provides new insights into how non-neuronal tissues contribute to behavioral plasticity. Our findings suggest that light-induced CYP-14A5 and CYP-dependent metabolic or signaling changes in the hypoderm may communicate with the nervous system to influence behavioral memory. This body-brain communication axis highlights the importance of systemic integration in mediating complex physiological and behavioral responses to environmental cues(Aghayeva et al., 2021; Fukuda et al., 2025; Liu et al., 2022; Zhang et al., 2018).

Beyond its biological significance, the light-inducible *cyp-14A5* promoter offers a useful new tool for gene expression studies in *C. elegans*. The ability to drive ectopic gene

262 expression in response to light provides a versatile system for temporally controlled
263 genetic manipulations. Our demonstration of light-induced sleep and mortality
264 phenotypes through ectopic gene expression illustrates the potential applications of this
265 tool in studying diverse biological processes in synthetic biology and physiology.
266 Previous studies have used heat shock or drug-inducible promoters for temporally
267 controlled gene expression in *C. elegans*(Monsalve et al., 2019; Stringham et al., 1992;
268 Wei et al., 2012). The light-inducible *cyp-14A5* promoter provides an alternative, simple-
269 to-implement approach and might be particularly useful when the drug-inducible system
270 is cumbersome, or heat shock effects are undesirable.

271 While our study uncovers a novel light-responding mechanism with functional
272 consequences in *C. elegans*, several limitations exist. First, the precise molecular
273 mechanism by which visible light activates ZIP-2 and/or CEBP-2 remains unclear, as
274 does the upstream signaling cascade linking light exposure to transcriptional activation.
275 Second, although we demonstrate a functional connection between light-induced *cyp-*
276 *14A5* expression and behavioral outcomes, the exact molecular interplay between
277 peripheral transcriptional changes and neural plasticity requires further exploration.
278 Finally, while the *cyp-14A5* promoter serves as a useful genetic tool, it does not confer
279 tissue specificity, and its ectopic effector expression requires control for light effects.
280 These limitations provide fertile ground for future research to build upon our findings.

281

282 **Materials & Methods**

283

284 ***C. elegans* strains**

285 *C. elegans* strains were grown on nematode growth media (NGM) plates seeded with
286 *Escherichia coli* OP50 at 20 °C with laboratory standard procedures unless otherwise
287 specified. The N2 Bristol strain was used as the reference wild type(Brenner, 1974).
288 Mutants and integrated transgenes were back-crossed at least five times. Genotypes of
289 strains used are as follows: *dmaIs156 IV [cyp-14A5p:: cyp-14A5::GFP; unc-*
290 *54p::mCherry]*, *agIs17 IV [irg-1p::gfp]*, *dmaEx [dpy-7p::cyp-14A5; myo-2p::mCherry],*
291 *dmaEx [cyp-14A5p::zip-10::mCherry; myo-2p::mCherry], dmaEx [cyp-14A5p::nlp-22;*
292 *myo-2p::mCherry], cebp-2 (tm5421) I, eif-2alpha(rog3) I, zip-2(tm4248) III, zip-2(ok3730)*
293 *III, cyp-14A5(gk152) V*.

294 PCR fusion constructs were used to generate transgenes(Hobert, 2002), using primer
295 sequences:

296 DM1310_*cyp-14A5*Pro c5p TCAACCACATCTTCCGATCA;
297 DM1311_*cyp-14A5*Pro to GFP c3p
298 CGACCTGCAGGCATGCAAGCTgatctttgttggacagaatagtttt;
299 DM2857_*dpy-7*p to *cyp-14A5* codutr Forward TGTCTCTGACGCCTGTGAGT;
300 DM2858_*dpy-7*p to *cyp-14A5* codutr Reverse
301 GATAAAGCAACGATGAAAACGCTCATTTTGTTTTCACAGAGCGGTAGA;
302 DM2944_*zip-2*uORF to *rpl-28*p-GOI-mCherry-5utr fusion F
303 CATCATAAAATAATTTATTTCCAGGTAAAATGTATCACGCAAAGACAACCACCG;
304 DM2945_*zip-2*uORF to *rpl-28*p-GOI-mCherry-5utr fusion
305 catgttatcttcttcacccttttgaggagccAAGCTCCCGTGGGAAGCTTGTG;
306 DM2948_*zip-10* to *cyp-14A5*p-GOI-mCherry-5utr fusion F

307 aaaactattctgtccaacaaagatcaaaATGACAACAATGACTAATTCTCTTATTTC;

308 DM2949_*zip-10* to *cyp-14A5*p-GOI-mCherry-5utr fusion R

309 catgttatcttcttcacccttttgaggagccGGAATGGTTGATTTGATTATTGAGTTG

310 DM2952_*nlp-22*cod::3utr to *cyp-14A5*p-GOI fusion

311 aaaactattctgtccaacaaagatcaaaATGCGTTCCATAATCGTCTTCATCG;

312 DM2953_*nlp-22*cod::3utr to *cyp-14A5*p-GOI fusion R cggttccactttctcatgagt

313

314 **Fluorescence microscopy and imaging**

315 SPE confocal (Leica) and epifluorescence microscopes were used to capture
316 fluorescence images. Animals were randomly picked at the same stage and treated with
317 1 mM levamisole in M9 solution (31742-250MG, Sigma-Aldrich), aligned on a 2% agar
318 pad on a slide for imaging. Identical setting and conditions were used to compare
319 experimental groups with control. For quantification of GFP fluorescence, animals were
320 outlined and quantified by measuring gray values using the ImageJ software. The data
321 were plotted and analyzed by using GraphPad Prism10.

322 For light-induced reporter imaging, reporter animals (synchronized young adults, 24 hrs
323 post L4) were exposed to white light (1500 Lux for 16 or 24 hrs, by Viribright 12-Watt, 800
324 Lumen, LED Desk Lamp Dimmable Office Lamp). For blue, green (SPE confocal, Leica),
325 and red light (HQRP 660 nm 14w LED pure red) conditions, animals of the same stage
326 were exposed to the same intensities (1500 Lux, 16 or 24 hours). Control groups from the
327 same batch of animals were maintained in darkness by opaque shields. Light intensities
328 and temperature were quantitatively measured by digital light meters and thermometers.

329

330 **RNA sequencing**

331 A synchronized population of wild-type young adult (24 hrs post L4) animals were
332 exposed to LED light (1500 lux, 24 hr duration, Viribright 12-Watt, 800 Lumen, LED Desk
333 Lamp Dimmable Office Lamp). Control groups from the same batch of animals were
334 maintained in darkness by opaque light shields. Four independent biological replicates
335 were used for both light-treated and control groups. For sample collection, the animals
336 were washed down from NGM plates using M9 solution and bacteria-cleaned with M9
337 washing in centrifuge tubes, homogenized by tissue disruptors and subjected to RNA
338 extraction using the RNeasy Mini Kit from Qiagen. 1 mg total RNA from each sample was
339 used for sequencing library construction. The libraries were constructed and sequenced
340 for paired end 150 bp by DNBseq (Innomics). The cleaned RNAseq reads were mapped
341 to the genome sequence of *C. elegans* using hisat2 and the mapped reads were assigned
342 to the genes using featureCounts(Kim et al., 2015; Liao et al., 2014). The abundance of
343 genes was expressed as RPKM (Reads per kilobase per million mapped reads) and
344 identification of differentially expressed genes (Table S1) was performed using the
345 DESeq2 package(Love et al., 2014).

346

347 ***C. elegans* behavioral assays**

348 The olfactory behavioral memory assay was as described previously with
349 modification(Chandra et al., 2023; Kauffman et al., 2010). Briefly, one day old adult worms
350 (24 hrs post L4) were washed with S basal buffer (0.1 M NaCl, 0.05 M K_3PO_4, pH 6.0) off

351 10 cm NGM plates and into microfuge tubes, where they were washed three times with
352 S basal buffer. The animals were split in two groups; one group was added to a microfuge
353 tube of S basal media and the other group was added to a microfuge tube of 1:10,000
354 dilution of butanone in S basal. The microfuge tubes were then rotated for 80 minutes.
355 The odor training includes three 80-minute cycles of training with odor, or a control buffer
356 interspersed with two 30-minute periods of feeding with OP50 *E. coli* bacteria. For
357 chemotaxis assay, 1 µL of (1 M) NaN_3 was pipetted onto the odor and diluent spots in 10
358 cm plastic petri dishes. 1 µL of 200 proof ethanol was added to the diluent spot and 1 µL
359 of 1:1000 butanone was added to the odor spot, while S basal or butanone-trained worms
360 were dropped onto the middle of 10 cm plastic petri dishes. The recovery period was
361 either under darkness or ambient light (approximately 600 Lux) for 16 hrs or were kept
362 under darkness for 2 or 4 hr periods followed by light exposure and chemotaxis to assay
363 behavioral memory.

364 For sleep analysis induced by *cyp-14A5p::nlp-22*, the bending angles, moving average
365 speed, and track length of *C. elegans* after 48 hours of exposure to either light or dark
366 conditions were analyzed using WormLab. In such experiment, a synchronized population
367 of young adult (24 hrs post L4) animals of indicated genotype or transgene expression
368 were used. After light exposure or control dark treatment, they were transferred to a fresh
369 NGM plate seeded with a small OP50 bacterial lawn and allowed to settle for at least ten
370 minutes to recover at room temperature. After the recovery period, a one-hour recording
371 session was conducted using WormLab. Bending angles were calculated as described in
372 the referenced method as a metric for sleep behaviors(Chandra et al., 2023). Moving
373 average speed was determined by tracking the displacement of the worms over time.

Statistics

Numerical data were analyzed using GraphPad Prism 10 Software (Graphpad, San Diego, CA) and presented as means ± S.D. unless otherwise specified, with *P* values calculated by unpaired two-tailed t-tests (comparisons between two groups), one-way ANOVA (comparisons across more than two groups) and two-way ANOVA (interaction between genotype and treatment), with post-hoc Tukey and Bonferroni's corrections. The lifespan assay was plotted and quantified using Kaplan–Meier lifespan analysis, and *P* values were calculated using the log-rank test.

Acknowledgment

Some strains were provided by the *Caenorhabditis* Genetics Center (CGC), which is funded by the NIH Office of Research Infrastructure Programs (P40 OD010440), and by Dr. E. Troemel. We also thank the *C. elegans* Reverse Genetics Core Facility (University of British Columbia), National Bioresource Project (S. Mitani, Tokyo Women's Medical University, Tokyo, Japan), Wormbase.org (NIH grant #U24 HG002223 to P. Sternberg), Wormatlas.org (NIH grant #OD010943 to D.H. Hall.), Aging Atlas (Dr. M. Wang) and CenGen (cengen.org) for their immensely helpful resources. The work was supported by NIH grants (R35GM139618 to D.K.M.), BARI Investigator Award (D.K.M.), and UCSF PBBR New Frontier Research Award (D.K.M.)

Author Contributions

D.K.M. designed and analyzed the *C. elegans* experiments, contributed to project conceptualization and wrote the manuscript. B.W. made the initial observation on *cyp-14A5* induction by light and performed RNAi screens and reporter imaging. Z.J. prepared RNA-seq samples and characterized light effects on the *cyp-14A5* reporter, cellular, behavioral and physiological phenotypes of various mutants with assistance from W.Y. and M.E. Y.L. analyzed the RNA-seq data. R.C. designed, performed and analyzed the behavioral memory assays. J.L. designed, performed and analyzed the light-induced sleep and phenoptotic aging assays. N.L., Y.L., B.W., Z.J., R.C., J.L. contributed to research materials, project conceptualization and editing manuscript.

Competing Interest Statement: The authors declare no competing interests.

413 **Figures and figure legends**

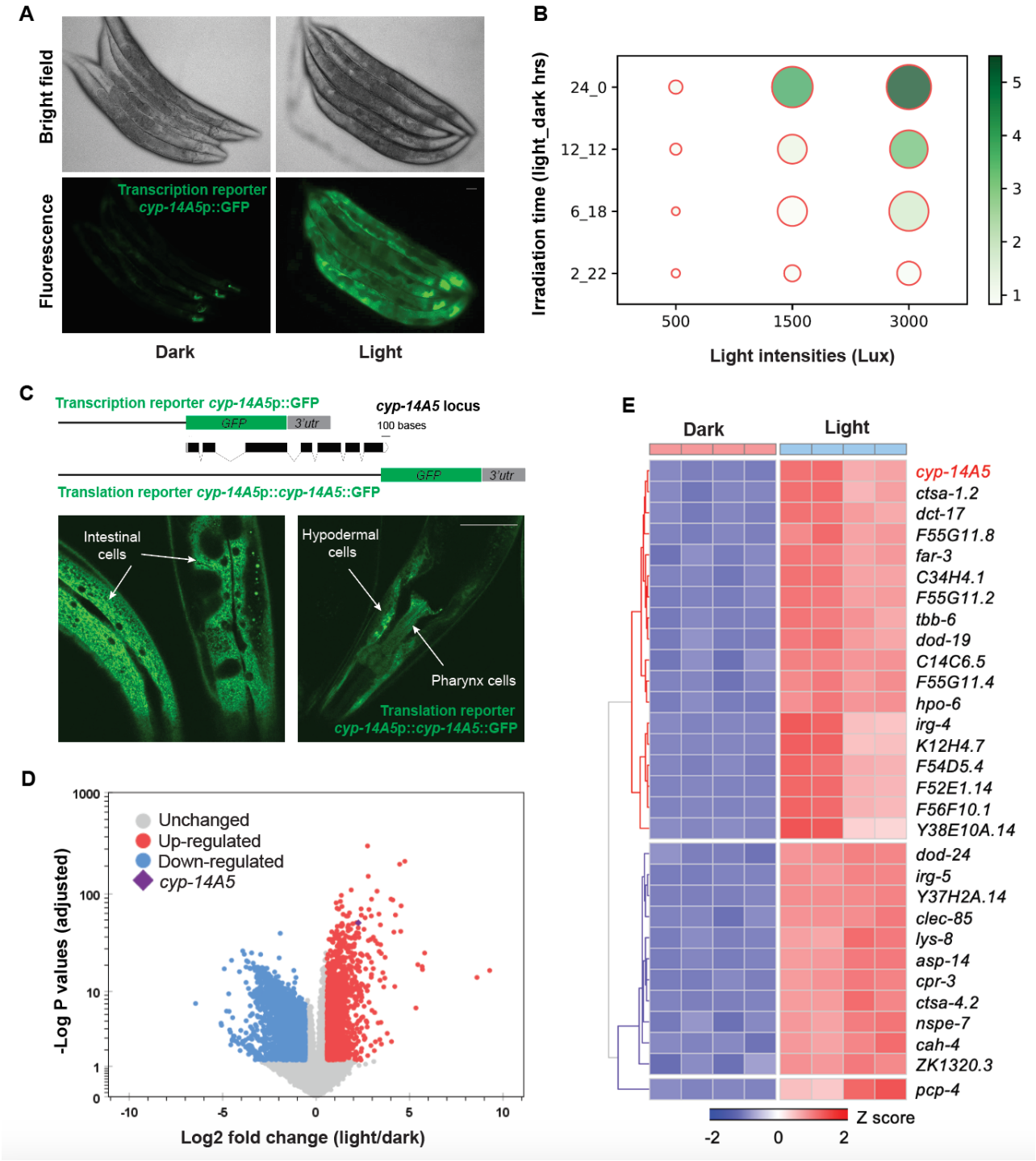

414

415 **Figure 1 Visible light exposure activates the CYP-encoding gene *cyp-14A5* in a**

416 **genetic program in *C. elegans***. A, Representative epifluorescence and brightfield

417 images showing *cyp-14A5*p::GFP induction by visible light exposure (1500 Lux, 24 hrs),
418 in synchronized young adults (24 hrs post L4). Scale bar: 50 µm. B, Bubble plot
419 showing fold induction of *cyp-14A5p::GFP* as a function of light intensity (Lux) and
420 duration (hours of light_dark indicated in Y axis). C, Schematic of *cyp-14A5*
421 transcriptional and translational GFP reporters. The translational reporter shows non-
422 neuronal (indicated by arrows) induction of CYP-14A5::GFP by light (1500 Lux, 24 hrs).
423 Scale bar: 50 µm. D, Volcano plot showing genes differentially regulated by light (1500
424 Lux, 24 hrs), with *cyp-14A5* highlighted, in synchronized young adults (24 hrs post L4).
425 E, Heat map of top-ranking visible light-regulated genes (top 30 including *cyp-14A5*).

426

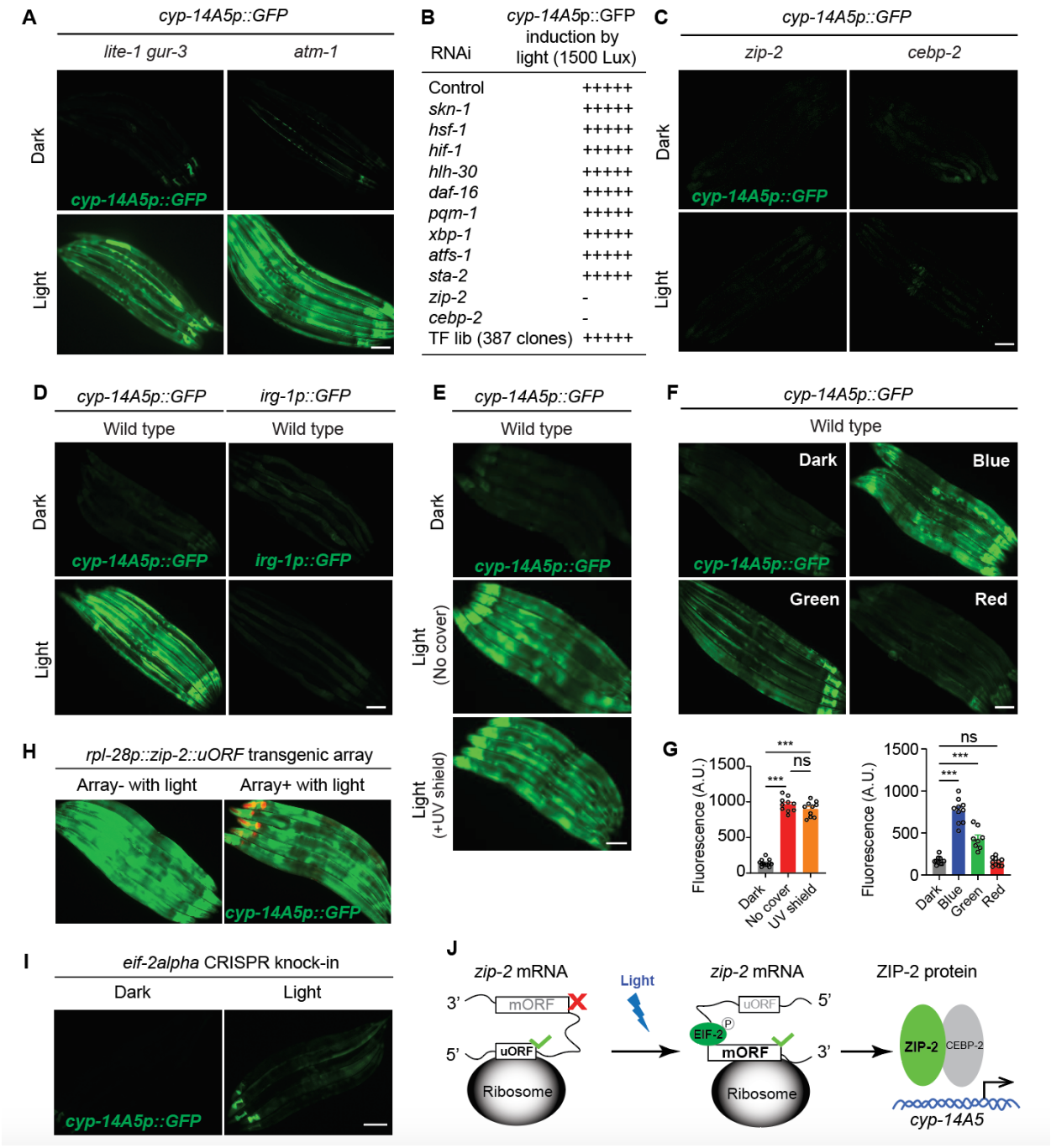

Figure 2 Light induction of *cyp-14A5*p::GFP requires the transcription factors ZIP-2 and CEBP-2. A, Representative epifluorescence images showing light-induced *cyp-14A5*p::GFP expression in *lite-1 gur-3* double and *atm-1* single loss-of-function mutants. Scale bar: 50 µm. B, Summary of RNAi screens identifying ZIP-2 and CEBP-2 as

432 essential transcriptional regulators of light-induced *cyp-14A5p::GFP* expression. C,
433 Representative epifluorescence images showing light-induced *cyp-14A5p::GFP*
434 expression in wild type, *zip-2* and *cebp-2* loss-of-function mutants. Scale bar: 50 μm. D,
435 Representative epifluorescence images showing light-induced *cyp-14A5p::GFP*
436 expression and no light-induced *irg-1p::GFP* expression in wild type animals. Scale bar:
437 50 μm. E, Representative epifluorescence images showing light-induced *cyp-*
438 *14A5p::GFP* expression unaffected by a UV shield. Scale bar: 50 μm. F, Representative
439 epifluorescence images showing light-induced *cyp-14A5p::GFP* expression by red,
440 green, blue LED light sources of equal intensities. Scale bar: 50 μm. G, Quantification of
441 E and F. *** indicates $P < 0.001$, n.s., non-significant. H, Representative
442 epifluorescence images showing light-induced *cyp-14A5p::GFP* expression unaffected
443 in *rpl-28p::zip-2uORF* transgenic animals. Scale bar: 50 μm. I, Representative
444 epifluorescence images showing light-induced *cyp-14A5p::GFP* expression abolished in
445 *eif-2alpha* mutants. Scale bar: 50 μm. J, Schematic model for light-induced transition of
446 *zip-2* mRNA from translating uORF to mORF, leading to increased ZIP-2 and
447 subsequent increased transcriptional *cyp-14A5* expression in cooperation with CEBP-2.
448 Other molecular players are omitted and uORF and mORF are separated for clarity.

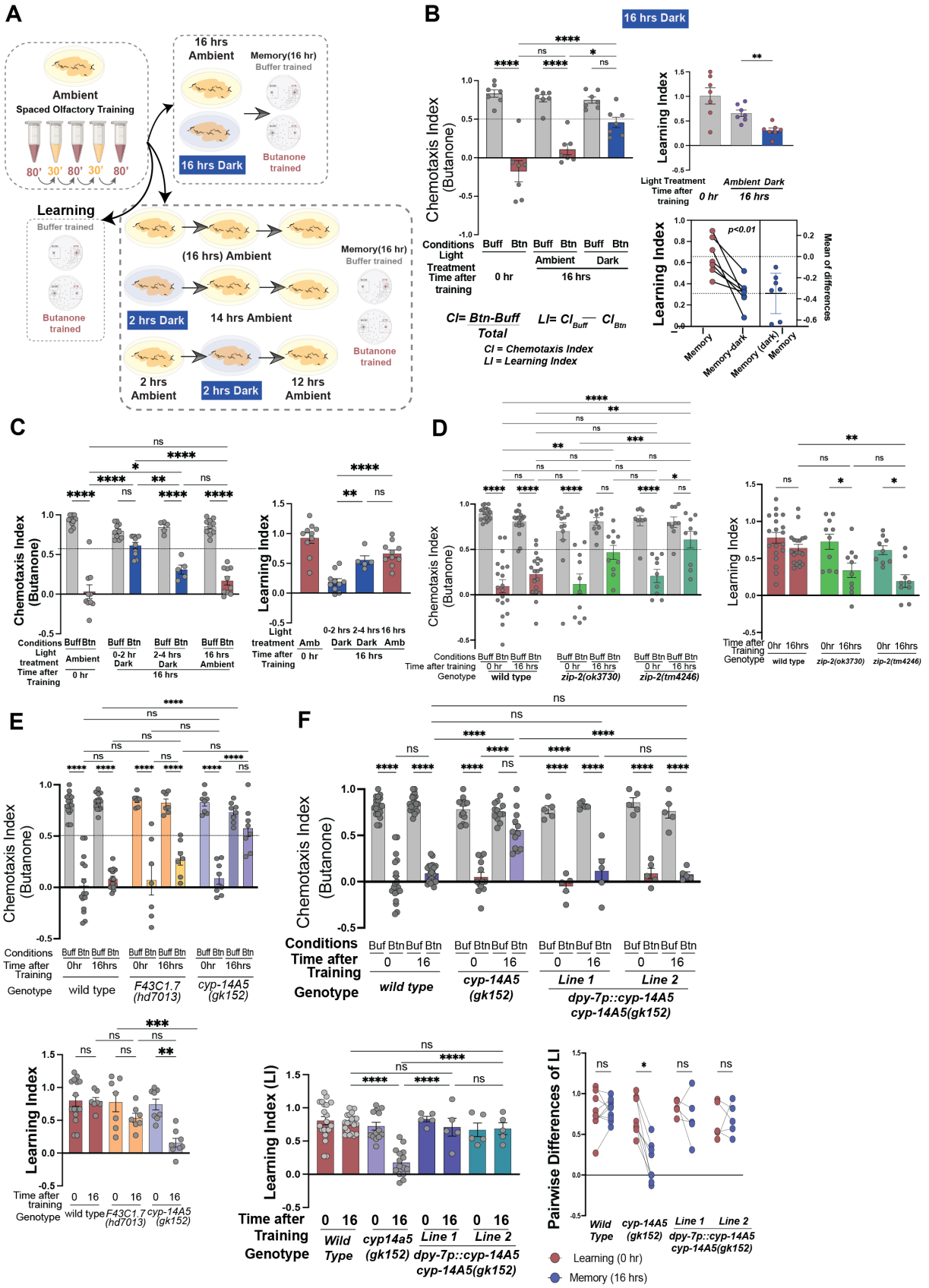
A
Ambient
Spaced Olfactory Training
80' 30' 80' 30' 80'
16 hrs Ambient
Memory(16 hr)
Buffer trained
16 hrs Dark
Butanone trained
Learning
Buffer trained
Butanone trained
(16 hrs) Ambient
Memory(16 hr)
Buffer trained
2 hrs Dark
14 hrs Ambient
Butanone trained
2 hrs Ambient
2 hrs Dark
12 hrs Ambient
B
16 hrs Dark
Chemotaxis Index (Butanone)
Conditions
Light Treatment
Time after training
Buff Btn Buff Btn Buff Btn
Ambient Dark
0 hr
16 hrs
CI= Btn-Buff / Total
LI= CI_Buff — CI_Btn
CI = Chemotaxis Index
LI = Learning Index
Learning Index
Light Treatment
Time after training
0 hr
Ambient Dark
16 hrs
p<0.01
Mean of differences
Memory
Memory-dark
Memory (dark)
Memory
C
Chemotaxis Index (Butanone)
Conditions
Light treatment
Time after Training
Buff Btn
Ambient
0 hr
0-2 hr Dark
2-4 hrs Dark
16 hrs Ambient
16 hrs
Learning Index
Light treatment
Time after Training
Amb
0 hr
0-2 hrs Dark
2-4 hrs Dark
16 hrs Amb
16 hrs
D
Chemotaxis Index (Butanone)
Conditions
Time after training
Genotype
Buff Btn
0 hr
16 hrs
wild type
zip-2(ok3730)
zip-2(tm4246)
Learning Index
Time after Training
Genotype
0hr 16hrs
wild type
zip-2(ok3730)
zip-2(tm4246)
E
Chemotaxis Index (Butanone)
Conditions
Time after Training
Genotype
Buff Btn
0hr 16hrs
wild type
F43C1.7 (hd7013)
cyp-14A5 (gk152)
Learning Index
Time after training
Genotype
0 16
wild type
F43C1.7 (hd7013)
cyp-14A5 (gk152)
F
Chemotaxis Index (Butanone)
Conditions
Time after Training
Genotype
Buf Btn
0 16
wild type
cyp-14A5 (gk152)
Line 1
Line 2
dpy-7p::cyp-14A5 cyp-14A5(gk152)
Learning Index (LI)
Time after Training
Genotype
0 16
Wild Type
cyp14a5 (gk152)
Line 1
Line 2
dpy-7p::cyp-14A5 cyp-14A5(gk152)
Pairwise Differences of LI
Wild Type
cyp-14A5 (gk152)
Line 1
Line 2
dpy-7p::cyp-14A5 cyp-14A5(gk152)
Learning (0 hr)
Memory (16 hrs)

450 **Figure 3 Light promotes behavioral plasticity and memory consolidation via a**
451 **ZIP-2/CYP axis in hypodermis**. A, Schematic of behavioral setup to test effects of
452 dark/light on olfactory memory. B, Wild-type learning and memory after 16 hours of dark
453 exposure. 7 trials, 50-200 animals per trial/condition. Two-way ANOVA shows
454 significant differences in chemotaxis (CI) under ambient light conditions (approximately
455 600 Lux) but not when the assay plates were placed in the dark. Learning (LI) indices
456 reflect the differences between buffer- and butanone-treated animals, attenuated under
457 dark (one-way ANOVA). Pairwise t-tests of the amount of memory retention under light
458 and dark recovery reveal the degree of memory loss under dark. C, Dark exposure
459 timeline shows that exposing animals to dark immediately after training (0-2 hr, Dark)
460 hampered memory retention, whereas dark conditions for the 2–4-hour period is less
461 sufficient to induce memory loss (two-way ANOVA). The lack of differences between
462 buffer and butanone-trained animals is reflected in the respective LIs (one-way
463 ANOVA). D, Two different loss-of-function alleles of *zip-2(tm4246)* or *zip-2(ok3730)* both
464 showed impaired memory, but learning remained intact (two-way ANOVA). 5-10 trials,
465 50-200 animals per trial/condition. E, Memory impairment of *cyp-14A5(gk152)* but not
466 *F43C1.7* null mutant animals (two-way ANOVA for CIs and One-way ANOVA for LIs. 7-
467 14 trials, 50-200 animals per trial/condition. F, Memory defects of *cyp-14A5(gk152)*
468 mutants are rescued by hypodermal expression of wild-type *cyp-14A5*. Two
469 independent transgenic lines show similar results with comparison of pairwise
470 differences in LIs and the amount of memory rescued by hypodermal *cyp-14A5* (Cis:
471 Two-way ANOVA; Lis: One-way ANOVA). * indicates $P < 0.05$, ** indicates $P < 0.01$, ***
472 indicates $P < 0.001$, **** indicates $P < 0.0001$, n.s., non-significant.

473

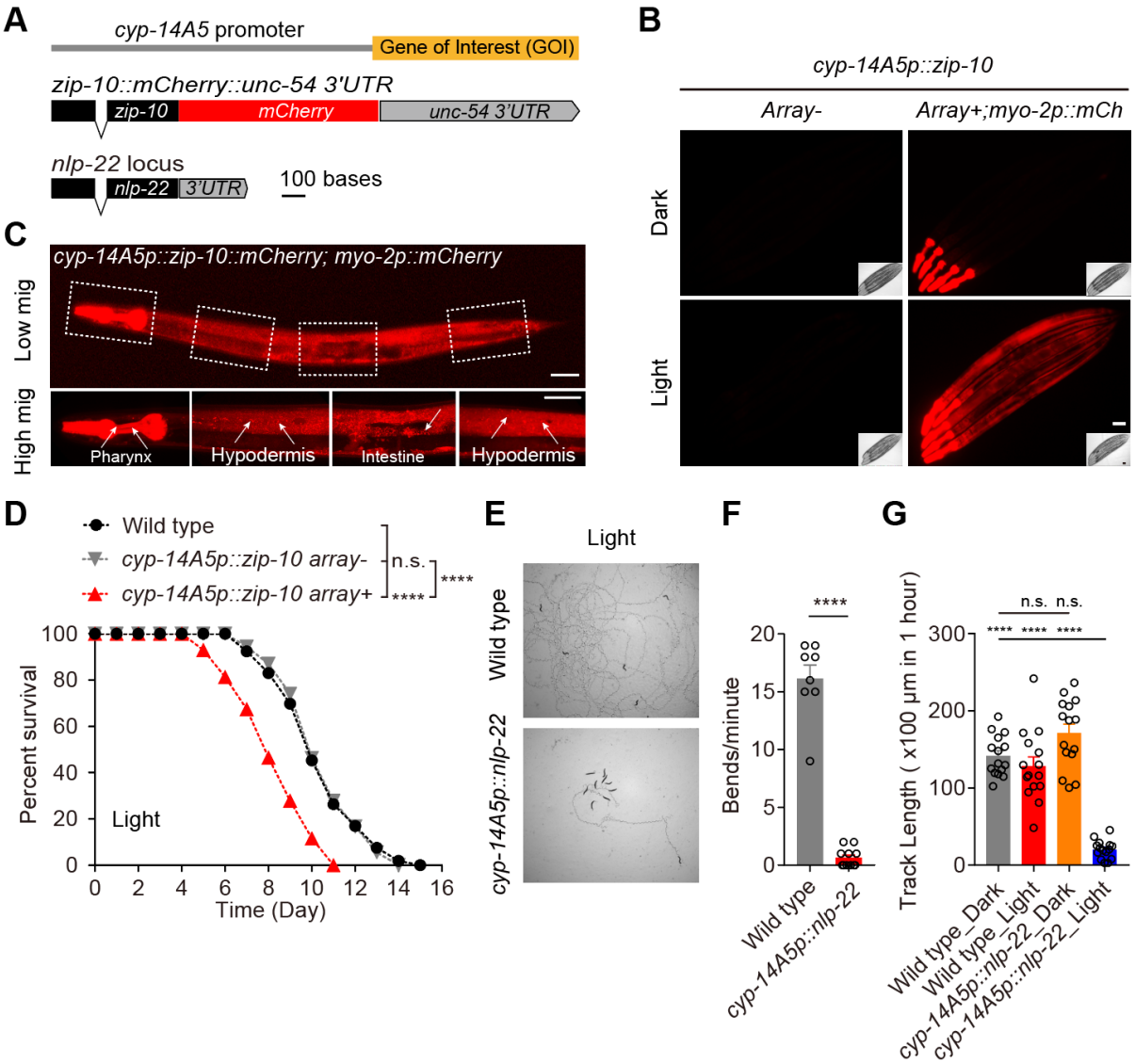

474

475 **Figure 4 Light-induced gene expression drives organismal phenotypes, including**

476 **sleep and shortened lifespans**. A, Schematic of synthetic constructs for light-inducible

477 *nlp-22* and *zip-10::mCherry* using the *cyp-14A5* promoter. B, Representative compound

478 epifluorescence images showing light-induced *cyp-14A5p::zip-10::mCherry* activation.

479 Scale bar: 50 µm. Pharyngeal muscle-specific *myo-2p::mCherry* was used as a co-

480 injection marker. C, Representative confocal fluorescence images showing light-induced
481 *cyp-14A5p::zip-10::mCherry* activation (1500 Lux, 24 hrs starting at 24 hrs post L4) in
482 major non-neuronal tissues (hypoderm, intestinal cells indicated by arrows). Scale bar:
483 50 μm. D, Representative lifespan curves showing that light-induced *zip-10* can
484 markedly shorten lifespan through transient light exposure (1500 Lux, 24 hrs starting at
485 24 hrs post L4). **** indicates $P < 0.0001$. E, Representative bright field images showing
486 quiescent sleep behaviors by light-induced *cyp-14A5p::nlp-22* expression through
487 transient light exposure (1500 Lux, 24 hrs starting at 24 hrs post L4). F, Quantification of
488 population bending frequencies for transient light-treated (1500 Lux, 24 hrs starting at
489 24 hrs post L4) control wild type and *cyp-14A5p::nlp-22* animals. G, Quantification of
490 population track lengths for control wild type and *cyp-14A5p::nlp-22* animals with
491 transient light (1500 Lux, 24 hrs starting at 24 hrs post L4) or darkness treatments. ***
492 indicates $P < 0.001$, **** indicates $P < 0.0001$, n.s., non-significant.

493

494

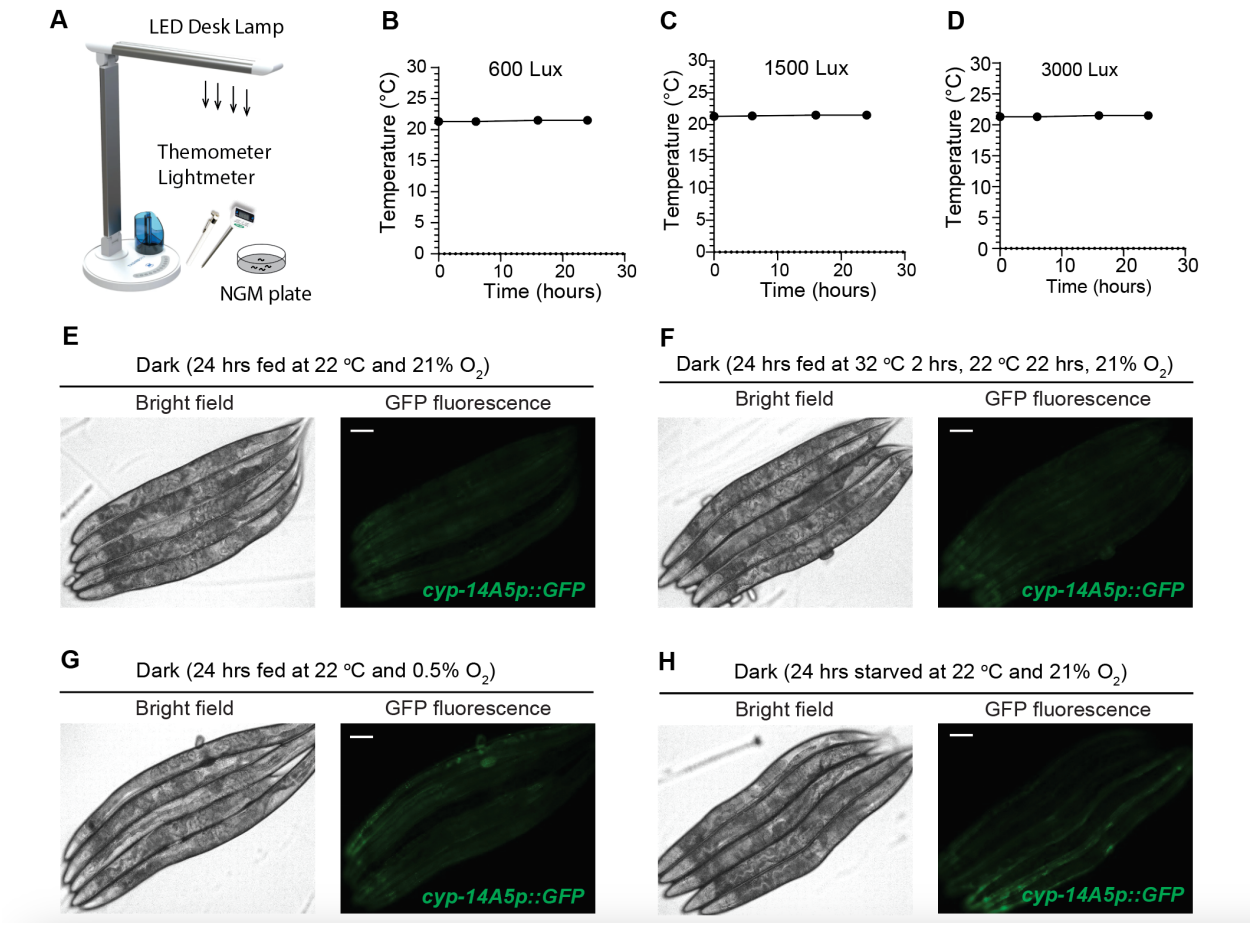

Figure S1 *cyp-14A5p::GFP* induction responds primarily to visible light exposure rather than changes in ambient oxygen, nutrient or temperature. A, Schematic of the setup for measurements of light intensity and temperature at a plane (in parallel to LED visible light sources) where animals are exposed to LED light in NGM plates. B, Measurements of temperature at the 600 Lux light intensity showing no change of temperature over 24 hrs. C, Measurements of temperature at the 1500 Lux light intensity showing no change of temperature over 24 hrs. D, Measurements of temperature at the 3000 Lux light intensity showing no change of temperature over 24 hrs. E-H, Representative bright-field and epifluorescence images showing no apparent

505 *cyp-14A5p::GFP* induction by transient exposure to heat shock (F), constant exposure

506 to 24 hrs of hypoxia (G) or starvation (H). Scale bar: 50 μm.

A

Gene ontology analysis
by WormCat:

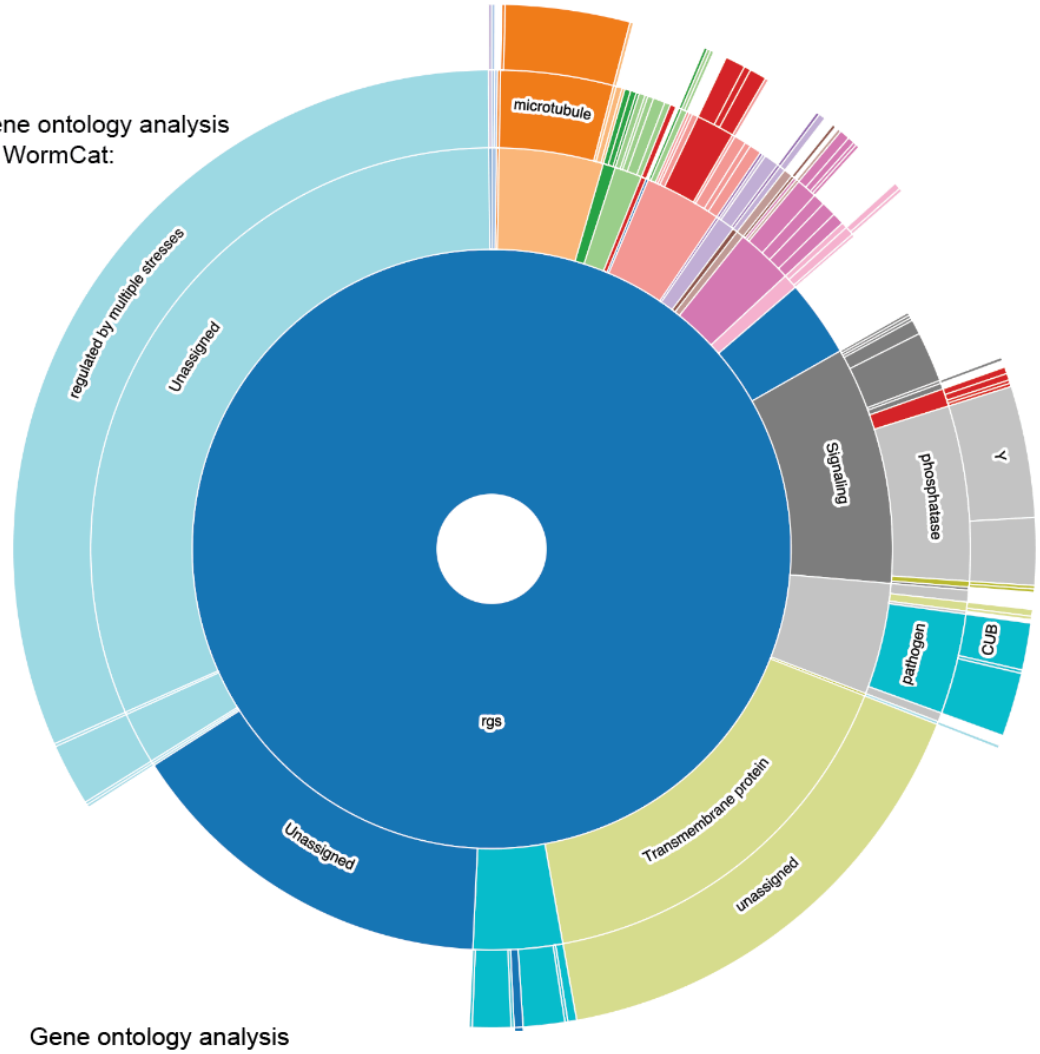

B Gene ontology analysis
by WormEnrichr:

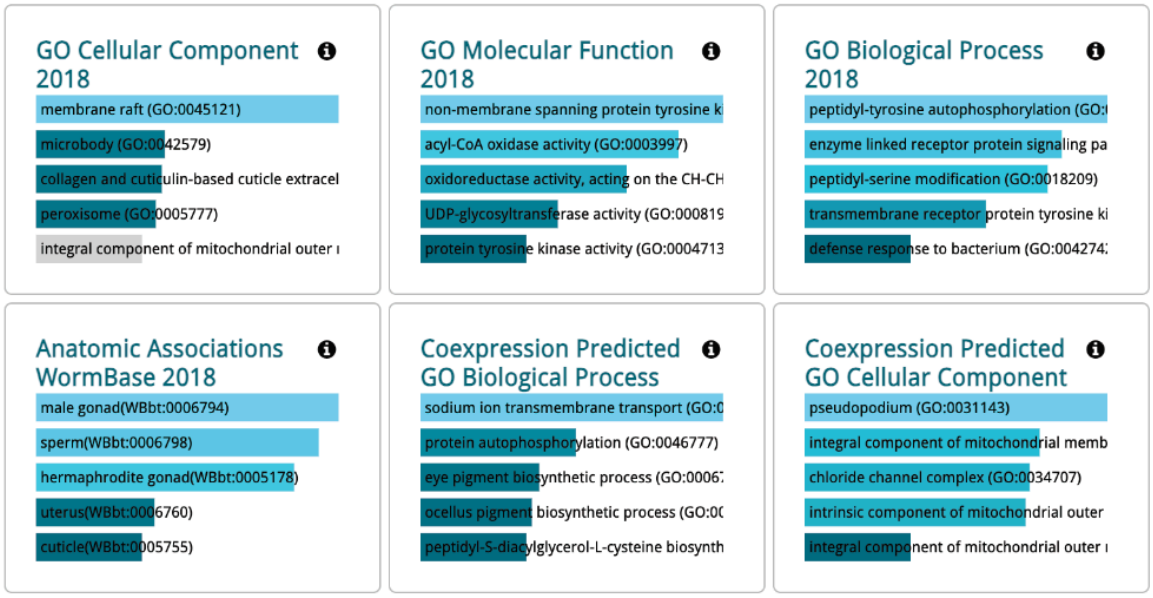

507

508 **Figure S2 Gene ontology analysis of light-induced transcriptomic changes.** A,
509 Starburst plot of gene ontology analysis of light-induced genes using WormCat
510 (http://www.wormcat.com/). B, Table summary of gene ontology analysis of light-
511 induced genes using WormEnrichr (https://maayanlab.cloud/WormEnrichr/).

512

513

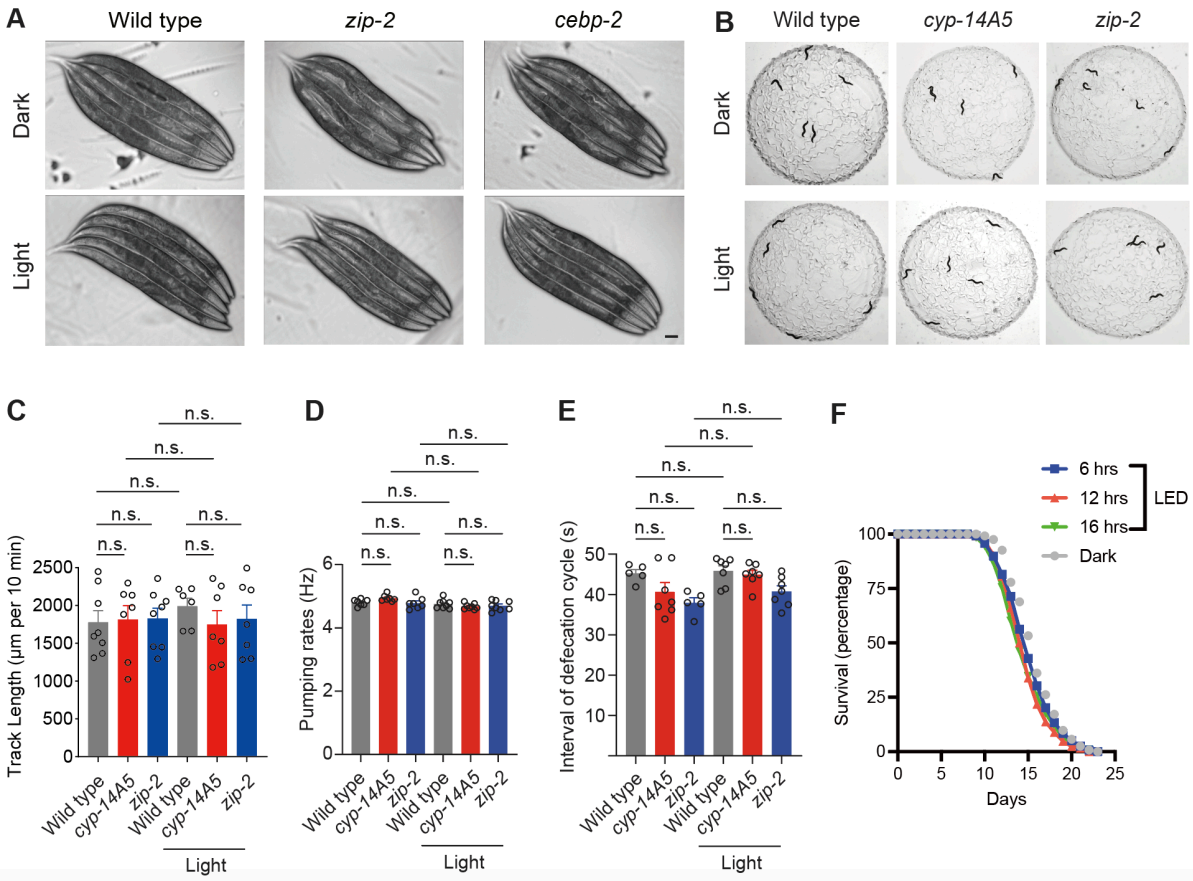

514

515 **Figure S3 No apparent effects of short-term transient visible LED light exposure**
516 **on development, morphology, simple behaviors and lifespans.** A, Representative
517 bright-field images showing no apparent effects of visible light exposure (1500 Lux, 24

518 hrs) on the body lengths and gross morphology of wild type, *cebp-2*, and *zip-2* loss-of-
519 function mutants. Scale bar: 50 μm. B. Representative images showing the movement
520 tracks of wild type, *cyp-14A5*, and *zip-2* loss-of-function mutants under dark and light
521 (1500 Lux, 24 hrs) conditions. C, Quantification of track lengths of wild type, *cyp-14A5*,
522 and *zip-2* loss-of-function mutants under dark and light (1500 Lux, 24 hrs) conditions. D,
523 Quantification of pumping rates of wild type, *cyp-14A5*, and *zip-2* loss-of-function
524 mutants under dark and light (1500 Lux, 24 hrs) conditions. E, Quantification of
525 defecation behaviors of wild type, *cyp-14A5*, and *zip-2* loss-of-function mutants under
526 dark and light (1500 Lux, 24 hrs) conditions. F, Lifespan curves of wild-type animals
527 under conditions of dark or transient LED light exposure for various indicated durations.

528

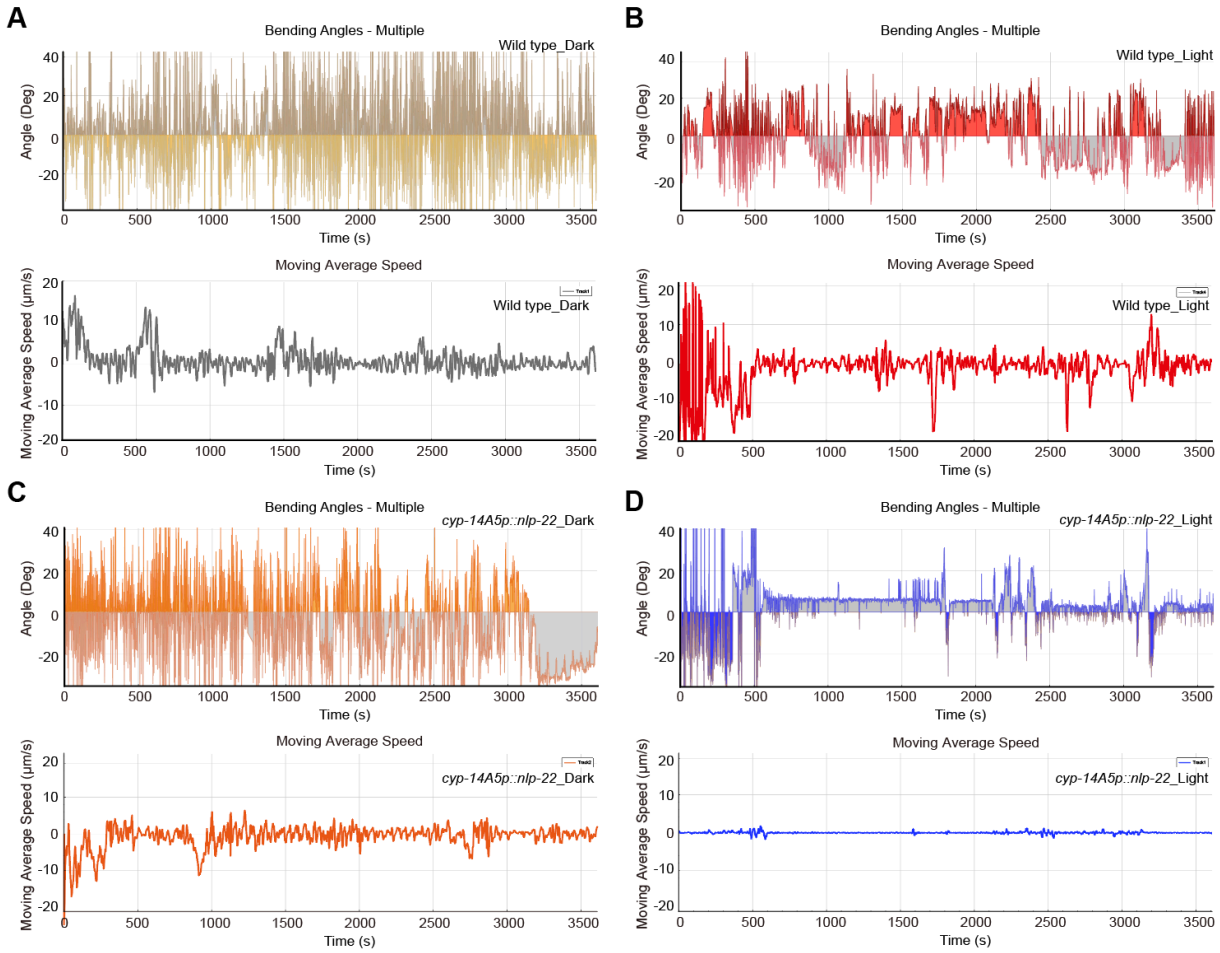

Figure S4 WormLab analysis reveals sleep bouts caused by light-induced *cyp-14A5p::nlp-22* expression. (A) Representative tracking of moving angles for body posture and average speed for control animals under dark conditions (N=15). (B) Representative tracking of moving angles for body posture and average speed for control animals after light exposure conditions (1500 Lux, 24 hrs, N=13). (C) Representative tracking of moving angles for body posture and average speed for *cyp-14A5p::nlp-22* transgenic animals under dark conditions (N=12). (B) Representative tracking of moving angles for body posture and average speed for *cyp-14A5p::nlp-22* transgenic animals after light exposure conditions (1500 Lux, 24 hrs, N=13).

539 ## References

540 Aghayeva U, Bhattacharya A, Sural S, Jaeger E, Churgin M, Fang-Yen C, Hobert O. 2021. DAF-16/FoxO
541 and DAF-12/VDR control cellular plasticity both cell-autonomously and via interorgan signaling.
542 *PLoS Biol* **19**:e3001204. doi:10.1371/journal.pbio.3001204
543 Andrabi M, Upton BA, Lang RA, Vemaraju S. 2023. An Expanding Role for Nonvisual Opsins in Extraocular
544 Light Sensing Physiology. *Annu Rev Vis Sci* **9**:245–267. doi:10.1146/annurev-vision-100820-
545 094018
546 Berson DM, Dunn FA, Takao M. 2002. Phototransduction by retinal ganglion cells that set the circadian
547 clock. *Science* **295**:1070–1073. doi:10.1126/science.1067262
548 Bhatla N, Horvitz HR. 2015a. Light and hydrogen peroxide inhibit C. elegans Feeding through gustatory
549 receptor orthologs and pharyngeal neurons. *Neuron* **85**:804–818.
550 doi:10.1016/j.neuron.2014.12.061
551 Bhatla N, Horvitz HR. 2015b. Light and hydrogen peroxide inhibit C. elegans Feeding through gustatory
552 receptor orthologs and pharyngeal neurons. *Neuron* **85**:804–818.
553 doi:10.1016/j.neuron.2014.12.061
554 Brenner S. 1974. The genetics of Caenorhabditis elegans. *Genetics* **77**:71–94.
555 Bringmann H. 2018. Sleep-Active Neurons: Conserved Motors of Sleep. *Genetics* **208**:1279–1289.
556 doi:10.1534/genetics.117.300521
557 Brito Querido J, Díaz-López I, Ramakrishnan V. 2024. The molecular basis of translation initiation and its
558 regulation in eukaryotes. *Nat Rev Mol Cell Biol* **25**:168–186. doi:10.1038/s41580-023-00624-9
559 Chandra R, Farah F, Muñoz-Lobato F, Bokka A, Benedetti KL, Brueggemann C, Saifuddin MFA, Miller JM,
560 Li J, Chang E, Varshney A, Jimenez V, Baradwaj A, Nassif C, Alladin S, Andersen K, Garcia AJ, Bi V,
561 Nordquist SK, Dunn RL, Garcia V, Tokalenko K, Soohoo E, Briseno F, Kaur S, Harris M, Guillen H,
562 Byrd D, Fung B, Bykov AE, Odisho E, Tsujimoto B, Tran A, Duong A, Daigle KC, Paisner R, Zuazo
563 CE, Lin C, Asundi A, Churgin MA, Fang-Yen C, Bremer M, Kato S, VanHoven MK, L'Étoile ND.
564 2023. Sleep is required to consolidate odor memory and remodel olfactory synapses. *Cell*
565 **186**:2911-2928.e20. doi:10.1016/j.cell.2023.05.006
566 Ciccia A, Elledge SJ. 2010. The DNA damage response: making it safe to play with knives. *Mol Cell*
567 **40**:179–204. doi:10.1016/j.molcel.2010.09.019
568 Costa-Mattioli M, Walter P. 2020. The integrated stress response: From mechanism to disease. *Science*
569 **368**:eaat5314. doi:10.1126/science.aat5314
570 Cronin TW, Johnsen S. 2016. Extraocular, Non-Visual, and Simple Photoreceptors: An Introduction to the
571 Symposium. *Integr Comp Biol* **56**:758–763. doi:10.1093/icb/icw106
572 De Magalhaes Filho CD, Henriquez B, Seah NE, Evans RM, Lapierre LR, Dillin A. 2018. Visible light reduces
573 C. elegans longevity. *Nat Commun* **9**:927. doi:10.1038/s41467-018-02934-5
574 Denisov IG, Makris TM, Sligar SG, Schlichting I. 2005. Structure and chemistry of cytochrome P450. *Chem*
575 *Rev* **105**:2253–2277. doi:10.1021/cr0307143
576 Do MTH, Yau K-W. 2010. Intrinsically photosensitive retinal ganglion cells. *Physiol Rev* **90**:1547–1581.
577 doi:10.1152/physrev.00013.2010
578 D'Orazio KN, Green R. 2021. Ribosome states signal RNA quality control. *Mol Cell* **81**:1372–1383.
579 doi:10.1016/j.molcel.2021.02.022
580 Dunbar TL, Yan Z, Balla KM, Smelkinson MG, Troemel ER. 2012. C. elegans detects pathogen-induced
581 translational inhibition to activate immune signaling. *Cell Host Microbe* **11**:375–386.
582 doi:10.1016/j.chom.2012.02.008

583 Edwards SL, Charlie NK, Milfort MC, Brown BS, Gravlin CN, Knecht JE, Miller KG. 2008. A novel molecular
584 solution for ultraviolet light detection in Caenorhabditis elegans. *PLoS Biol* **6**:e198.
585 doi:10.1371/journal.pbio.0060198
586 Estes KA, Dunbar TL, Powell JR, Ausubel FM, Troemel ER. 2010. bZIP transcription factor zip-2 mediates
587 an early response to Pseudomonas aeruginosa infection in Caenorhabditis elegans. *Proc Natl*
588 *Acad Sci U S A* **107**:2153–2158. doi:10.1073/pnas.0914643107
589 Fukuda A, Sato K, Fujimori C, Yamashita T, Takeuchi A, Ohuchi H, Umatani C, Kanda S. 2025. Direct
590 photoreception by pituitary endocrine cells regulates hormone release and pigmentation.
591 *Science* **387**:43–48. doi:10.1126/science.adj9687
592 Genuth NR, Barna M. 2018. Heterogeneity and specialized functions of translation machinery: from
593 genes to organisms. *Nat Rev Genet* **19**:431–452. doi:10.1038/s41576-018-0008-z
594 Gong J, Yuan Y, Ward A, Kang L, Zhang B, Wu Z, Peng J, Feng Z, Liu J, Xu XZS. 2016. The C. elegans Taste
595 Receptor Homolog LITE-1 Is a Photoreceptor. *Cell* **167**:1252-1263.e10.
596 doi:10.1016/j.cell.2016.10.053
597 Hanson SM, Scholüke J, Liewald J, Sharma R, Ruse C, Engel M, Schüler C, Klaus A, Arghittu S, Baumbach
598 F, Seidenthal M, Dill H, Hummer G, Gottschalk A. 2023. Structure-function analysis suggests that
599 the photoreceptor LITE-1 is a light-activated ion channel. *Curr Biol* **33**:3423-3435.e5.
600 doi:10.1016/j.cub.2023.07.008
601 Hattar S, Lucas RJ, Mrosovsky N, Thompson S, Douglas RH, Hankins MW, Lem J, Biel M, Hofmann F,
602 Foster RG, Yau K-W. 2003. Melanopsin and rod-cone photoreceptive systems account for all
603 major accessory visual functions in mice. *Nature* **424**:76–81. doi:10.1038/nature01761
604 Hobert O. 2002. PCR fusion-based approach to create reporter gene constructs for expression analysis in
605 transgenic C. elegans. *Biotechniques* **32**:728–730. doi:10.2144/02324bm01
606 Kauffman AL, Ashraf JM, Corces-Zimmerman MR, Landis JN, Murphy CT. 2010. Insulin signaling and
607 dietary restriction differentially influence the decline of learning and memory with age. *PLoS Biol*
608 **8**:e1000372. doi:10.1371/journal.pbio.1000372
609 Keller J, Ellieva A, Ma DK, Ju J, Nehk E, Konkel A, Falck JR, Schunck W-H, Menzel R. 2014. CYP-13A12 of
610 the nematode Caenorhabditis elegans is a PUFA-epoxygenase involved in behavioural response
611 to reoxygenation. *Biochem J* **464**:61–71. doi:10.1042/BJ20140848
612 Kim D, Langmead B, Salzberg SL. 2015. HISAT: a fast spliced aligner with low memory requirements. *Nat*
613 *Methods* **12**:357–360. doi:10.1038/nmeth.3317
614 Kniazeva M, Ruvkun G. 2025. Translation elongation defects activate the Caenorhabditis elegans ZIP-2
615 bZIP transcription factor-mediated toxin defense. *Proc Natl Acad Sci U S A* **122**:e2423578122.
616 doi:10.1073/pnas.2423578122
617 Liao Y, Smyth GK, Shi W. 2014. featureCounts: an efficient general purpose program for assigning
618 sequence reads to genomic features. *Bioinformatics* **30**:923–930.
619 doi:10.1093/bioinformatics/btt656
620 Liebel F, Kaur S, Ruvolo E, Kollias N, Southall MD. 2012. Irradiation of skin with visible light induces
621 reactive oxygen species and matrix-degrading enzymes. *J Invest Dermatol* **132**:1901–1907.
622 doi:10.1038/jid.2011.476
623 Liu Y, Zhou J, Zhang N, Wu X, Zhang Q, Zhang W, Li X, Tian Y. 2022. Two sensory neurons coordinate the
624 systemic mitochondrial stress response via GPCR signaling in C. elegans. *Dev Cell* **57**:2469-
625 2482.e5. doi:10.1016/j.devcel.2022.10.001
626 Love MI, Huber W, Anders S. 2014. Moderated estimation of fold change and dispersion for RNA-seq
627 data with DESeq2. *Genome Biol* **15**:550. doi:10.1186/s13059-014-0550-8
628 Lucas RJ, Hattar S, Takao M, Berson DM, Foster RG, Yau K-W. 2003. Diminished pupillary light reflex at
629 high irradiances in melanopsin-knockout mice. *Science* **299**:245–247.
630 doi:10.1126/science.1077293

631 Ma DK, Rothe M, Zheng S, Bhatla N, Pender CL, Menzel R, Horvitz HR. 2013. Cytochrome P450 drives a
632 HIF-regulated behavioral response to reoxygenation by C. elegans. *Science* **341**:554–558.
633 doi:10.1126/science.1235753
634 Ma Z, Horrocks J, Mir DA, Cox M, Ruzga M, Rollins J, Rogers AN. 2023. The integrated stress response
635 protects against ER stress but is not required for altered translation and lifespan from dietary
636 restriction in Caenorhabditis elegans. *Front Cell Dev Biol* **11**:1263344.
637 doi:10.3389/fcell.2023.1263344
638 Mahmoud BH, Ruvolo E, Hexsel CL, Liu Y, Owen MR, Kollias N, Lim HW, Hamzavi IH. 2010. Impact of
639 long-wavelength UVA and visible light on melanocompetent skin. *J Invest Dermatol* **130**:2092–
640 2097. doi:10.1038/jid.2010.95
641 Mir DA, Ma Z, Horrocks J, Rogers A. 2024. Stress-Induced Eukaryotic Translational Regulatory
642 Mechanisms. *J Clin Med Sci* **8**:1000277.
643 Monsalve GC, Yamamoto KR, Ward JD. 2019. A New Tool for Inducible Gene Expression in
644 Caenorhabditis elegans. *Genetics* **211**:419–430. doi:10.1534/genetics.118.301705
645 Nelson MD, Trojanowski NF, George-Raizen JB, Smith CJ, Yu C-C, Fang-Yen C, Raizen DM. 2013. The
646 neuropeptide NLP-22 regulates a sleep-like state in Caenorhabditis elegans. *Nat Commun*
647 **4**:2846. doi:10.1038/ncomms3846
648 Neve EPA, Ingelman-Sundberg M. 2010. Cytochrome P450 proteins: retention and distribution from the
649 endoplasmic reticulum. *Curr Opin Drug Discov Devel* **13**:78–85.
650 Pandey T, Ma DK. 2022. Stress-Induced Phenoptosis: Mechanistic Insights and Evolutionary Implications.
651 *Biochemistry (Mosc)* **87**:1504–1511. doi:10.1134/S0006297922120082
652 Reddy KC, Dunbar TL, Nargund AM, Haynes CM, Troemel ER. 2016. The C. elegans CCAAT-Enhancer-
653 Binding Protein Gamma Is Required for Surveillance Immunity. *Cell Rep* **14**:1581–1589.
654 doi:10.1016/j.celrep.2016.01.055
655 Schuch AP, Moreno NC, Schuch NJ, Menck CFM, Garcia CCM. 2017. Sunlight damage to cellular DNA:
656 Focus on oxidatively generated lesions. *Free Radic Biol Med* **107**:110–124.
657 doi:10.1016/j.freeradbiomed.2017.01.029
658 Shi Y, Zhang J, Li X, Han Y, Guan J, Li Yilin, Shen J, Tzvetanov T, Yang D, Luo X, Yao Y, Chu Z, Wu T, Chen Z,
659 Miao Y, Li Yufei, Wang Q, Hu J, Meng J, Liao X, Zhou Y, Tao L, Ma Y, Chen J, Zhang M, Liu R, Mi Y,
660 Bao J, Li Z, Chen X, Xue T. 2024. Non-image-forming photoreceptors improve visual orientation
661 selectivity and image perception. *Neuron* S0896-6273(24)00840–7.
662 doi:10.1016/j.neuron.2024.11.015
663 Sinha A, Rae R, Iatsenko I, Sommer RJ. 2012. System wide analysis of the evolution of innate immunity in
664 the nematode model species Caenorhabditis elegans and Pristionchus pacificus. *PLoS One*
665 **7**:e44255. doi:10.1371/journal.pone.0044255
666 Sinha NK, McKenney C, Yeow ZY, Li JJ, Nam KH, Yaron-Barir TM, Johnson JL, Huntsman EM, Cantley LC,
667 Ordureau A, Regot S, Green R. 2024. The ribotoxic stress response drives UV-mediated cell
668 death. *Cell* **187**:3652-3670.e40. doi:10.1016/j.cell.2024.05.018
669 Stringham EG, Dixon DK, Jones D, Candido EP. 1992. Temporal and spatial expression patterns of the
670 small heat shock (hsp16) genes in transgenic Caenorhabditis elegans. *Mol Biol Cell* **3**:221–233.
671 doi:10.1091/mbc.3.2.221
672 Troemel ER, Chu SW, Reinke V, Lee SS, Ausubel FM, Kim DH. 2006. p38 MAPK regulates expression of
673 immune response genes and contributes to longevity in C. elegans. *PLoS Genet* **2**:e183.
674 doi:10.1371/journal.pgen.0020183
675 Van der Auwera P, Frooninckx L, Buscemi K, Vance RT, Watteyne J, Mirabeau O, Temmerman L, De Haes
676 W, Fancsalszky L, Gottschalk A, Raizen DM, Nelson MD, Schoofs L, Beets I. 2020. RPamide
677 neuropeptides NLP-22 and NLP-2 act through GnRH-like receptors to promote sleep and
678 wakefulness in C. elegans. *Sci Rep* **10**:9929. doi:10.1038/s41598-020-66536-2

679 Van Gelder RN. 2008. Non-visual photoreception: sensing light without sight. *Curr Biol* **18**:R38-39.
680 doi:10.1016/j.cub.2007.11.027
681 Wang C, Long Y, Wang B, Zhang C, Ma DK. 2023. GPCR signaling regulates severe stress-induced
682 organismic death in Caenorhabditis elegans. *Aging Cell* **22**:e13735. doi:10.1111/acel.13735
683 Wei X, Potter CJ, Luo L, Shen K. 2012. Controlling gene expression with the Q repressible binary
684 expression system in Caenorhabditis elegans. *Nat Methods* **9**:391–395. doi:10.1038/nmeth.1929
685 Wong D, Bazopoulou D, Pujol N, Tavernarakis N, Ewbank JJ. 2007. Genome-wide investigation reveals
686 pathogen-specific and shared signatures in the response of Caenorhabditis elegans to infection.
687 *Genome Biol* **8**:R194. doi:10.1186/gb-2007-8-9-r194
688 Zhang B, Gong J, Zhang W, Xiao R, Liu J, Xu XZS. 2018. Brain-gut communications via distinct
689 neuroendocrine signals bidirectionally regulate longevity in C. elegans. *Genes Dev* **32**:258–270.
690 doi:10.1101/gad.309625.117
691